DOI: 10.1002/ejic.201001257

Facile Oxidative Addition of Organic Halides to Heteroleptic and Homoleptic Pd^0–N-Heterocyclic Carbene Complexes

Jung-Hyun Lee,[a] Hyeong-Tak Jeon,[a] Yong-Joo Kim,*[a] Kyung-Eun Lee,[b] Young Ok Jang,[b] and Soon W. Lee[b]

Keywords: Palladium / Oxidative addition / N-Heterocyclic carbenes / Halides / Heteroleptic complexes

Novel heteroleptic Pd^0 complexes with an N-heterocyclic carbene (NHC) ligand [$(Me_3P)Pd(NHC)$] (NHC = IPr, **1**; SIPr, **2**) were obtained from [$Pd(CH_2{=}CHPh)(PMe_3)_2$] and an equivalent of NHC [NHC = 1,3-bis(2,6-diisopropylphenyl)-imidazol-2-ylidene (IPr) or 1,3-bis(2,6-diisopropylphenyl)-4,5-dihydroimidazol-2-ylidene (SIPr)]. Further treatments of complexes **1** and **2** with an additional equimolar NHC afforded the corresponding bis(NHC)–Pd^0 complexes [$Pd(NHC)_2$] (NHC = IPr, **3**; SIPr, **4**). Complexes **1**–**4** readily reacted with dichloromethane or chloroform to give C–Cl oxidative addition products. In addition, the reactivity of complex **2** toward other organic halides such as bromobenzene, *trans*-1,2-dichloroethylene, and 5,5′-dibromo-2,2′-bithiophene to produce the corresponding oxidative addition products was investigated. Finally, the ligand replacement of complex **1** with a chelating phosphane was examined.

Introduction

Pd–NHC-catalyzed (NHC=N-heterocyclic carbene) C–C or C–X (X = heteroatom) coupling reactions have been increasingly studied during the past decade.[1–4] In the catalytic cycles, the oxidative addition of organic halides is a fundamental step to give organic products or Pd–σ-bonded intermediates. Although many low-valent group 10 metal–phosphane complexes undergo oxidative addition with organic halides,[5–9] quite a few Pd^0–NHC complexes exhibit such reactivity.[10–12] For example, Cavell's[11] group as well as the groups of Caddick and Cloke[12] reported the oxidative addition of aryl halides to Pd^0–NHC complexes. In addition, the groups of Cavell[11b] and Radius[13] demonstrated oxidative additions of organic halides and sulfides to Ni^0–NHC complexes. Theoretical and mechanistic studies on the oxidative addition of aryl halides to Pd^0–NHC complexes were also reported.[14,15]

The NHC ligand is known to be an alternative group of typical tertiary phosphanes in zero-valent Pd complexes. In addition, the activity of the Pd–NHC-catalyzed cross-couplings varies with the electronic or steric properties of ancillary ligands, and it also depends on the stability or reactivity of the catalysts. To develop efficient catalysts other than known Pd–NHC catalysts, we tried to prepare novel NHC–Pd^0 complexes from dialkyl–Pd complexes, which may serve as precursors for zero-valent Pd complexes. We here report the preparation of several phosphane–NHC–Pd^0 and bis(NHC)–Pd^0 complexes and demonstrate their oxidative addition reactivity toward various organic halides including halogenated solvents.

[a] Department of Chemistry, Kangnung-Wonju National University,
Gangneung 210-702, South Korea
Fax: +82-33-640-2264
E-mail: yjkim@ kangnung.ac.kr
[b] Department of Chemistry, Sungkyunkwan University, Natural Science Campus,
Suwon 440-746, Korea

Results and Discussion

Preparation of PMe_3–NHC–Pd^0 Complexes

Room-temperature reactions of [$Pd(CH_2{=}CHPh)(PMe_3)_2$],[16,17] which could be generated in situ from *trans*-[$PdEt_2L_2$] and styrene, with IPr [IPr = 1,3-bis(2,6-diisopropylphenyl)imidazol-2-ylidene] or SIPr [1,3-bis(2,6-diisopropylphenyl)-4,5-dihydroimidazol-2-ylidene] in a 1:1 molar ratio gave novel PMe_3–NHC–Pd^0 complexes [$(Me_3P)Pd(NHC)$] (NHC = IPr, **1**; SIPr, **2**) (Scheme 1). As mentioned in the Introduction, the above NHC ligands were adopted as supporting ligands to the Pd center in our study.

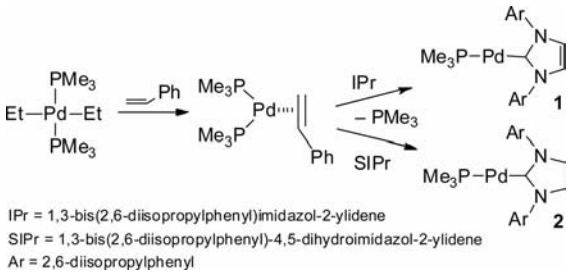

Scheme 1.

Complexes **1** and **2** were obtained as pale yellow solids, which were moderately stable in the solid state at room temperature but air sensitive in solution. In particular, these complexes slowly decomposed in polar solvents and readily reacted with halogenated solvents (see Scheme 4 below). The ^{1}H and ^{31}P{^{1}H} NMR spectra of the final products indicate that these contained a small amount of the bis(carbene)–Pd^0 complexes [Pd(NHC)$_2$] [NHC = IPr (**3**) or SIPr (**4**)],[17] which were presumably formed by the dissociation of PMe_3 during the reaction. As a result, an analytically pure product could not be obtained. Moreover, during the course of recrystallization in ditheyl ether or THF, complexes **1** and **2** partially dissociated the PMe_3 ligand to give the bis(NHC)–Pd^0 complexes **3** and **4** (Scheme 2). A similar phosphane dissociation was also previously observed in the reactions between [Pd{P(*o*-tolyl)$_3$}$_2$] and IPr, SIPr, or 1,3-bis(adamantly)imidazolin-2-ylidene to give phosphane–NHC–Pd^0 complexes [(R$_3$P)Pd(NHC)] [NHC = IPr, SIPr; PR$_3$ = P(*o*-tol)$_3$] or bis(NHC)–Pd^0 complexes.[18,19] Recently, Nolan and co-workers[20] reported a general synthetic route to phosphane–NHC–Pd^0 complexes, [(R$_3$P)-Pd(NHC)] [NHC = IPr, SIPr; PR$_3$ = PPh$_3$, PCy$_3$, P(Bu)(Ad)$_2$], from [(NHC)Pd(η^3-allyl)Cl] and tertiary phosphanes. The ^{13}C{^{1}H} NMR spectrum of **1** shows a doublet ($J_{P,C}$ = 16 Hz) at δ = 178.5 ppm due to the N*C*N carbene carbon, which indicates that the PMe_3 ligand in complex **1** exerts a stronger *trans* influence than other phosphanes ($J_{P,C}$ = 83–94 Hz) in the above-mentioned phosphane–NHC–Pd complexes.

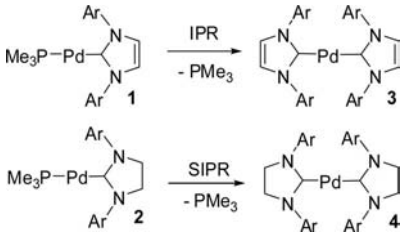

Scheme 2.

To confirm the formation of bis(NHC)–Pd^0 complexes, complexes **1** and **2** were treated with one additional equivalent of the NHC agent (Scheme 2), and complexes **3** and **4** were obtained as yellow (64%) and orange (46%) crystals, respectively. Consistent with our expectation, the NMR (^{1}H, ^{13}C{^{1}H}, and ^{31}P{^{1}H} NMR) spectroscopic data of complexes **3** and **4** agree well with those previously reported.[18]

We also examined the reactivity of bis(phosphane)–diethyl–Pd^{II} complexes toward NHC ligands, as shown in Scheme 3. In these reactions, one PMe_3 ligand was replaced with the NHC ligand, and NHC–diethyl–Pd^{II} complexes *trans*-[Pd(PMe$_3$)Et$_2$(IPr)] (**5**) and *trans*-[Pd(PMe$_3$)Et$_2$(SIPr)] (**6**) were obtained. *trans*- or *cis*-diethyl–Pd^{II} complexes that possess tertiary phosphanes are known to decompose by β-H elimination or reductive elimination.[21] The starting material, *trans*-[PdEt$_2$(PMe$_3$)$_2$][16b] is thermally unstable in solid and in solution at room temperature. However, in this work, we could prepare unique NHC-stabilized bis(diethyl)–Pd^{II} complexes that are moderately stable both in the solid state and in solution at room temperature. We monitored the ^{1}H NMR spectra of compounds **5** and **6** dissolved in THF or toluene by heating the solutions from room temperature to 70 °C. The solutions were thermally stable to 50 °C. When the temperature was raised to 70 °C, decomposition of the compounds occurred. However, we could not identify PMe$_3$–NHC–Pd^0 compounds due to their complicated spectral patterns. These results strongly support the known fact that NHC ligands behave as better stabilizing ancillary ligands than tertiary phosphane ligands. Complexes **5** and **6** were isolated as white crystals, and the molecular structure of complex **6** in Figure 1 was determined by X-ray diffraction. The crystal and refinement data of **6** is summarized in Table 1. The coordination sphere of Pd can be described as a square plane that consists of one NHC, one PMe_3, and two *trans*-Et ligands. The N1–C1 [1.345(2) Å] and N2–C1 [1.355(2) Å] bonds, in which C1 is the carbene carbon, are significantly shorter than the other N–C bonds [the average is 1.460(2) Å]. The shortening of the N–C (carbene) bonds probably reflects the resonance of those bonds due to the lone pair of electrons on the carbene carbon. Terminal methyl groups on the ethyl ligands are

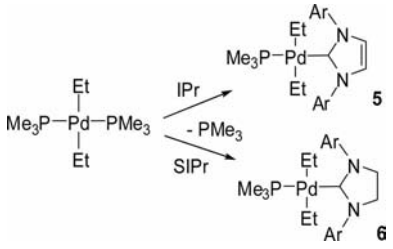

Scheme 3.

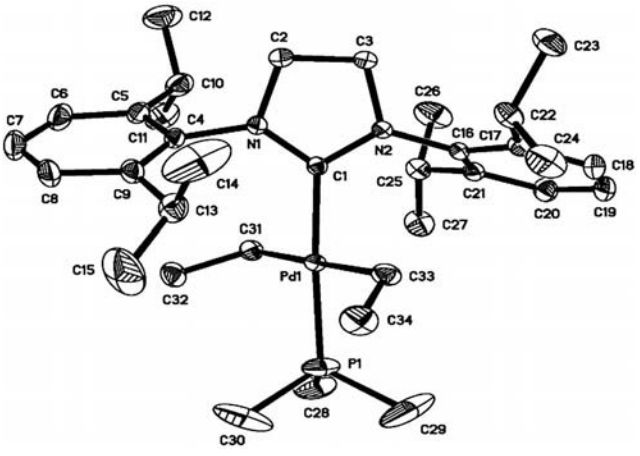

Figure 1. ORTEP drawing of **6**. Selected bond lengths [Å] and angles [°]: Pd1–C1 2.027(2), Pd1–C31 2.135(2), Pd1–C33 2.144(2), Pd1–P1 2.2533(7), N1–C1 1.345(2), N(1)–C4 1.446(2), N1–C2 1.478(3), N2–C1 1.355(2), N2–C16 1.439(2), N2–C3 1.475(3); C1–Pd1–C31 90.44(8), C1–Pd1–C33 88.60(8), C31–Pd1–C33 179.01(9), C1–Pd1–P1 176.22(6), C31–Pd1–P1 90.25(6), C33–Pd1–P1 90.73(7), N1–C1–N2 106.3(2), C1–N1–C2 112.8(2), C1–N2–C3 112.5(2).

Table 1. Crystal data and structure refinements for complexes **6**–**8**, **10**, and **11**–**15**.

	6	**7**	**8**	**10**	**11**·Et_2O
Formula	$C_{34}H_{57}N_2PPd$	$C_{31}H_{47}Cl_2N_2P_1Pd$	$C_{31}H_{49}Cl_2N_2PPd$	$C_{55}H_{78}Cl_2N_4Pd$	$C_{58}H_{82}Cl_2N_4OPd$
M_r	631.19	655.98	657.99	972.51	1028.58
T [K]	296(2)	296(2)	296(2)	200(2)	200(2)
Crystal size [mm^3]	0.42 × 0.38 × 0.32	0.40 × 0.30 × 0.20	0.52 × 0.44 × 0.36	0.32 × 0.25 × 0.22	0.25 × 0.20 × 0.13
Crystal system	orthorhombic	monoclinic	monoclinic	triclinic	orthorhombic
Space group	*Pbca*	$P2_1/n$	$P2_1/n$	$P\bar{1}$	$P2_12_12_1$
a [Å]	18.9961(3)	11.3708(1)	11.3636(5)	12.3144(8)	12.9601(7)
b [Å]	15.7425(2)	20.5091(2)	20.7074(9)	12.3951(7)	20.4366(11)
c [Å]	23.3332(4)	14.3001(2)	14.2241(6)	17.2209(10)	21.3284(11)
α [°]				82.391(1)	
β [°]		91.596(1)	91.459(2)	87.649(2)	
γ [°]				88.439(1)	
V [Å^3]	6977.7(2)	3333.56(6)	3346.0(3)	2602.6(3)	5649.0(5)
Z	8	4	4	2	4
$d_{calcd.}$ [g cm^{-3}]	1.202	1.307	1.306	1.241	1.209
μ [mm^{-1}]	0.600	0.786	0.783	0.498	0.463
$F(000)$	2688	1368	1376	1032	2184
T_{min}	0.7866	0.7439	0.6862	0.8570	0.8929
T_{max}	0.8311	0.8586	0.7657	0.8984	0.9422
Measured reflections	116702	51129	45489	19369	42254
Unique reflections	8699	8278	8142	12619	13825
R(int) reflections [$I > 2\sigma(I)$]	6937	6685	6807	5657	7956
Parameters refined	343	334	335	559	595
Max. $\Delta\rho$ [e Å^{-3}]	0.421	0.309	0.399	2.022	1.099
Min. $\Delta\rho$ [e Å^{-3}]	–0.326	–0.268	–0.337	–1.185	–1.866
GoF on F^2	1.100	1.012	1.031	0.887	0.985
R_1[a]	0.0318	0.0269	0.0251	0.0678	0.0575
wR_2[b]	0.0686	0.0632	0.0622	0.1155	0.0804
R (all data)	0.0468	0.0392	0.0344	0.1568	0.1372
wR_2[a] (all data)	0.0793	0.0694	0.0677	0.1509	0.1099

	12	**13**	**14**·C_6H_{14}	**15**	
Formula	$C_{36}H_{52}BrN_2PPd$	$C_{32}H_{49}Cl_2N_2PPd$	$C_{72}H_{112}Br_2N_4P_2Pd_2S_2$	$C_{54}H_{52}P_4Pd$	
M_r	631.19	670.00	1556.36	931.24	
T [K]	296(2)	296(2)	200(2)	200(2)	
Crystal size [mm^3]	0.26 × 0.16 × 0.10	0.20 × 0.16 × 0.12	0.17 × 0.15 × 0.04	0.21 × 0.18 × 0.17	
Crystal system	monoclinic	monoclinic	triclinic	monoclinic	
Space group	$P2_1/c$	$P2_1/c$	$P\bar{1}$	$C2/c$	
a [Å]	12.9802(7)	13.8695(5)	10.543(1)	18.2610(7)	
b [Å]	15.5482(8)	23.4601(8)	10.875(1)	13.2898(6)	
c [Å]	17.9521(8)	20.8522(7)	17.851(2)	20.0819(8)	
α [°]			84.535(3)		
β [°]	100.257(2)	92.265(2)	85.478(3)	109.419(1)	
γ [°]			69.365(3)		
V [Å^3]	3565.2(3)	6779.6(4)	1904.4(4)	4596.3(3)	
Z	4	8	1	4	
$d_{calcd.}$ [g cm^{-3}]	1.360	1.313	1.357	1.346	
μ [mm^{-1}]	1.712	0.775	1.660	0.579	
$F(000)$	1512	2800	808	1928	
T_{min}	0.6645	0.8605	0.7656	0.8881	
T_{max}	0.8475	0.9128	0.9366	0.9080	
Measured reflections	32723	100790	14201	16453	
Unique reflections	8510	16421	9236	5582	
R(int) reflections [$I > 2\sigma(I)$]	5050	7055	3505	3736	
Parameters refined	371	685	373	267	
Max. $\Delta\rho$ [e Å^{-3}]	0.409	0.373	0.653	0.623	
Min. $\Delta\rho$ [e Å^{-3}]	–0.399	–0.612	–1.141	–0.699	
GoF on F^2	0.958	0.943	0.761	0.955	
R_1[a]	0.0407	0.0517	0.0581	0.0405	
wR_2[b]	0.0625	0.0877	0.0789	0.0729	
R (all data)	0.0998	0.1749	0.1693	0.0811	
wR_2[a] (all data)	0.0752	0.1187	0.1106	0.0890	

[a] $R_1 = \Sigma||F_o| - |F||/\Sigma|F_o|$. [b] $wR_2 = \Sigma[w(F_o^2 - F_c^2)^2]/\Sigma[w(F_o^2)^2]^{1/2}$.

oriented perpendicular to the square plane that contains the NHC ligand. The Pd–C bond lengths [2.135(2) and 2.144(2) Å] in complex **6** are somewhat longer than those found for other Pd–dialkyl complexes: 2.089(3) and 2.090(3) Å in *cis*-[$PdMe_2(PPh_2Me)$];[22] 2.026 and 2.029 Å in [$PdMe_2(Me_2NCH_2CH_2NMe_2)$];[23] and 2.087(4) Å in

[PdMe$_2$(Me$_2$PCH$_2$CH$_2$PMe$_2$)].[23] However, we could not provide a clear explanation due to the limited structural data available for *trans*-dialkyl–Pd complexes.

Reactivity of PMe$_3$–NHC–Pd^0 Complexes toward Halogenated Solvents (Dichloromethane and Chloroform)

Attempts to recrystallize PMe$_3$–NHC–Pd^0 complexes **1** and **2** from halogenated solvents such as CH_2Cl_2 or $CHCl_3$ failed because these complexes reacted with those solvents (Scheme 4).

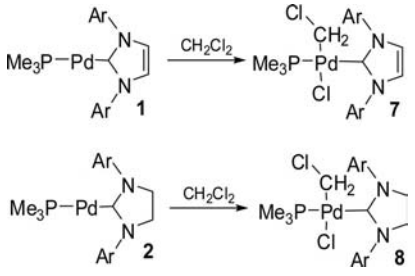

Scheme 4.

When complex **1** or **2** was dissolved in CH_2Cl_2 at room temperature, white solids of [(Me$_3$P)ClPd(CH$_2$Cl)(IPr)] (**7**, 84%) or [(Me$_3$P)ClPd(CH$_2$Cl)(SIPr)] (**8**, 69%) were obtained. These reactions also occurred in the presence of either a stoichiometric or an excess amount of CH_2Cl_2 in organic solvents. However, in spite of several attempts in $CHCl_3$, pure products could not be obtained because they were thermally unstable and inseparable mixtures. Complexes **7** and **8** were characterized by ^{1}H, ^{13}C{^{1}H}, and ^{31}P{^{1}H} NMR spectroscopy, elemental analyses, as well as X-ray diffraction.

The methylene signals (Pd–C*H*$_2$Cl) in the ^{1}H NMR spectra of **7** and **8** in $CDCl_3$ at –40 °C appeared at δ = 3.08 and 3.14 ppm, respectively, as a doublet ($J_{P,H}$ = 7.3 Hz), which are comparable to the typical C*H*$_2$X signals; for example, those in *trans*-[PdCl(CH$_2$Cl){P(*t*Bu)$_2$H}$_2$][24] (δ = 3.73 ppm in C_6D_6 at 298 K) and *trans*-[PdCl(CH$_2$Cl)(PPh$_3$)$_2$][25] (δ = 3.92 ppm in C_6D_6 at 298 K). A singlet in the ^{31}P{^{1}H} NMR spectra of complexes **7** and **8** support the presence of one PMe_3 ligand coordinated to the Pd center. The doublets ($J_{P,C}$ = 158 and 147 Hz) at 183.6 (**7**) and 209.8 ppm (**8**) due to the carbene carbon (N*C*N) in the ^{13}C NMR spectra indicate the *trans* orientation of the carbene (NHC) and the PMe_3 ligands.

As shown in Figure 2, the methine signals C*H*(CH$_3$)$_2$ of the 2,6-diisopropylphenyl groups on the imidazoline ring of **7** exhibit temperature dependence in the range of –40 to 20 °C in $CDCl_3$. At –40 °C, the methine signals in the *i*Pr$_2$ and *i*Pr′$_2$ groups split into two septets at δ = 2.78 and 3.26 ppm. This phenomenon arises because the *i*Pr groups do not interchange by the phenyl-ring rotation at this temperature.

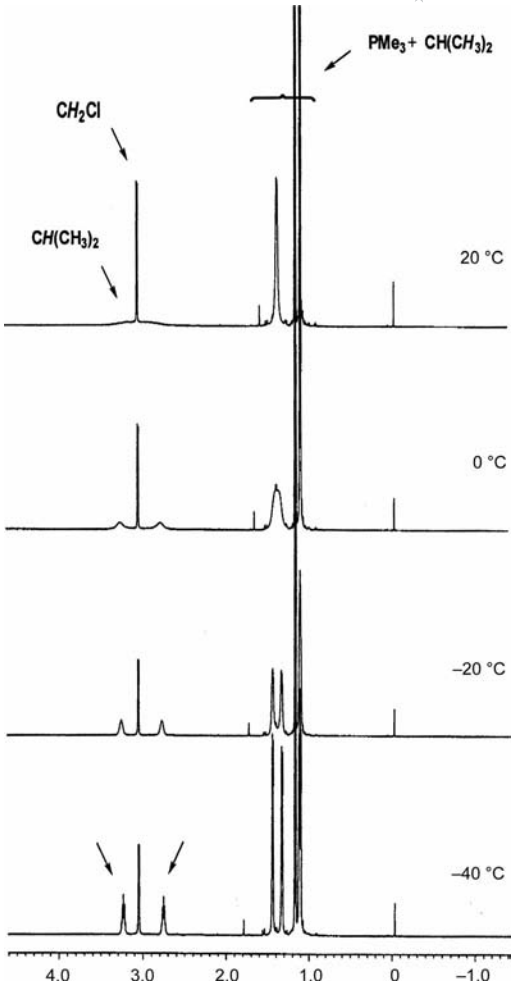

Figure 2. Variable-temperature ^{1}H NMR (600 MHz) spectroscopic signals for the alkyl substituents of **7** from –40 to 20 °C in $CDCl_3$.

At around 0 °C, the methine signals becme broad. At 20 °C, a complete broadening of the methine signals occurs, and the signals can be hardly identified. This type of peak broadening is also observed for the methyl protons of the *i*Pr and *i*Pr′ groups. Two well-separated doublets (δ = 1.36 and 1.47 ppm) due to the methyl protons colalesce at 0 °C. In the coalescence temperature range, ^{1}H NMR spectra of **7** were carefully taken as a function of temperature at 2 °C intervals to find out the exact coalescence temperature (T_c). As a result, we could determine the coalescence temperatures 22 °C for the methine (C*H*) and –1 °C for the methyl signals of CH(C*H*$_3$)$_2$ of the 2,6-diisopropylphenyl groups, respectively. At these temperatures, the free energies for activation barriers were calculated from the Eyring equation [$\Delta G^{\ddagger}$ = 19.12 T_c(10.32 + log T_c – log k_c); k_c = $\pi\Delta\nu/\sqrt{2}$; $\Delta\nu$ = the chemical shift difference in hertz between two separate signals].[26] The $\Delta G^{\ddagger}$ value for the rotation of the methine groups in $CDCl_3$ is (13.5 ± 0.10) kJ mol^{-1} and that of the methyl groups is (13.2 ± 0.10) kJ mol^{-1}.

The organic substituents of complex **7** were characterized by heteronuclear multiple quantum coherence (HMQC), COSY(H–H), NOESY, and distortionless enhancement by

polarization rransfer (DEPT) NMR spectroscopic techniques.

X-ray crystal structures (see Figures 3 and 4) confirm the formation of complexes **7** and **8**. Because these complexes are isostructural, only the structure of complex **7** is described in detail. In Figure 3 (complex **7**), the coordination sphere Pd1 can be described as a square plane, with the Cl and CH_2Cl ligands being *trans* to each other. The imidazoline ring is significantly twisted from the two 2,6-bis(isopropyl)phenyl rings with the dihedral angle of 73.54(6) or 78.16(7)°, probably because of the two bulky isopropyl substituents on the phenyl rings. The Pd–C (Pd–CH_2Cl) bond lengths [Pd1–C31: 2.021(2) Å in **7**; 2.018(2) Å in **8**] are close to that [2.031(2) Å] of *trans*-[PdCl(CH_2Cl)(PPh_3)$_2$],[25] which was prepared from [$PdCl_2$(cod)] (cod = 1,2-cyclooctadiene), excess amounts of diazomethane or bis(chloromethyl)mercury, followed by the ligand replacement with PPh_3. Although many cases of the thermal or photoinduced oxidative addition of dihalomethanes to low-valent Pt,[27–30] Pd,[24,31–33] Rh,[34–43] Ru,[44] Ir,[45–47] Co,[48] and Au[49] complexes were reported, only a few cases have been known to date for zero-valent Pd complexes, including [Pd(P*t*Bu$_2$H)$_3$],[24] [Pd(PCy_3)$_2$(dba)] (dba = dibenzylideneacetone; Cy = cyclohexyl),[31] and [PdN($CH_2CH_2PPh_2$)$_3$].[28] Furthermore, there have been no reports for the structural characterization of the oxidative addition complex Cl–PdCH_2Cl by X-ray diffraction. Complexes **7** and **8** provide the first examples of oxidative addition of dichloromethane to Pd^0–NHC complexes.

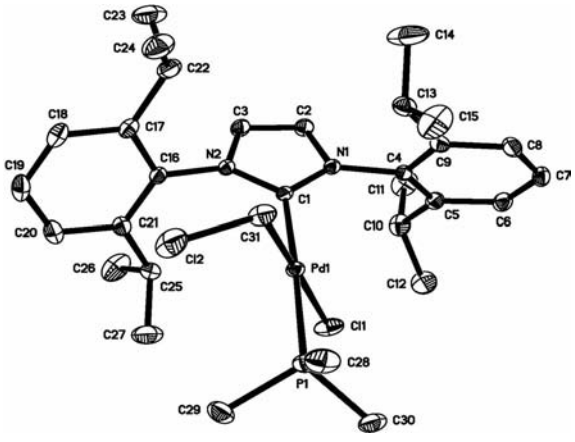

Figure 3. ORTEP drawing of **7**. Selected bond lengths [Å] and angles [°]: Pd1–C31 2.021(2), Pd1–C1 2.055(2), Pd1–P1 2.3031(5), Pd1–Cl1 2.3831(5), Cl2–C31 1.817(2), N1–C1 1.362(2), N1–C2 1.382(2), N1–C4 1.448(2), N2–C1 1.360(2), N2–C3 1.383(2), N2–C16 1.449(2); C31–Pd1–C1 91.23(7), C31–Pd1–P1 90.27(6), C1–Pd1–P1 176.97(5), C31–Pd1–Cl1 179.08(7), Cl2–C31–Pd1 113.61(12).

The bis(NHC)–Pd^0 complexes (NHC = IPr, **3**; SIPr, **4**) also react with halogenated solvents (Scheme 5). In the case of CH_2Cl_2, rapid oxidative addition occurs to produce the corresponding addition products, [ClPd(CH_2Cl)(IPr)$_2$] (**9**) and [ClPd(CH_2Cl)(SIPr)$_2$] (**10**), the formation of which can readily be monitored by the color change from the initial orange to colorless. The methylene signals (CH_2Cl) in the

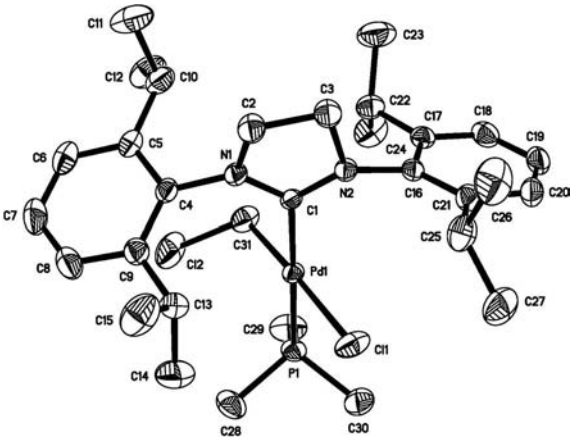

Figure 4. ORTEP drawing of **8**. Selected bond lengths [Å] and angles [°]: Pd1–C31 2.018(2), Pd1–C1 2.059(1), Pd1–P1 2.3112(4), Pd1–Cl1 2.3828(5), Cl2–C31 1.822(2), N1–C1 1.341(2), N1–C2 1.475(2), N1–C4 1.441(2), N2–C1 1.346(2), N2–C16 1.441(2), N2–C3 1.477(2), C2–C3 1.495(3); C31–Pd1–C1 91.38(7), C31–Pd1–P1 89.96(6), C1–Pd1–P1 177.78(4), C31–Pd1–Cl1 177.86(6), Cl2–C31–Pd1 113.1(1).

^{1}H NMR spectra of **9** and **10** appear at δ = 3.05 and 3.07 ppm as a singlet, respectively. In sharp contrast, complex **3** reacted with chloroform to produce dichloro–NHC–Pd^{II} species [Pd(IPr)$_2$Cl$_2$] (**11**) in 79% yield. In this reaction, chloroform served as a chlorine source. Although we have no concrete evidence about the side products, we speculate that the product may have been formed by oxidative addition of $CHCl_3$, followed by the C–Cl cleavage at some stage. Molecular structures of **10** (Figure 5) and **11** (Figure 6) were determined by X-ray diffraction. The coordination sphere of **10** can be described as square planar, and the Cl and CH_2Cl ligands are *trans* to each other.

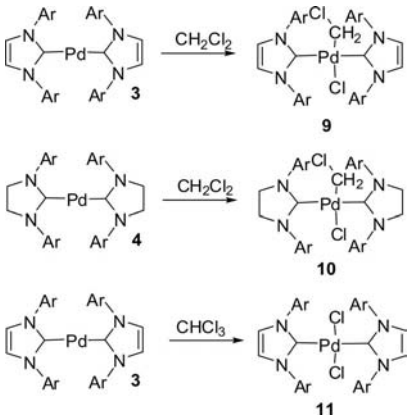

Scheme 5.

The five-membered rings in the NHC ligands are significantly twisted from the molecular plane. The coordination sphere of **11** is also square-planar with a set of *trans*-chlorido ligands and a set of *trans*-NHC ligands.

Various organic halides readily undergo oxidative addition to electronically unsaturated Pd^0 complexes.[5] In this study, small organic halogenated molecules such as dichloromethane or chloroform oxidatively add to the phos-

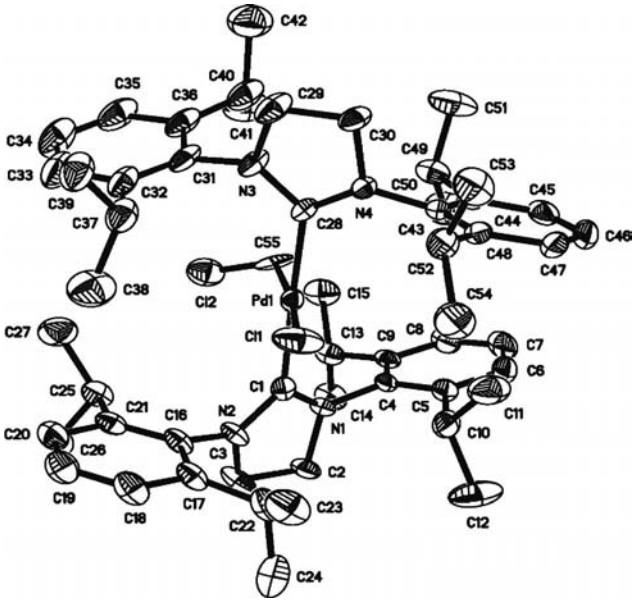

Figure 5. ORTEP drawing of **10**. Selected bond lengths [Å] and angles [°]: Pd1–C28 2.056(5), Pd1–C1 2.080(6), Pd1–C55 2.115(5), Pd1–Cl1 2.393(2), Cl2–C55 1.554(6); C28–Pd1–C1 178.3(2), C28–Pd1–C55 94.2(2), C1–Pd1–C55 86.6(2), C28–Pd1–Cl1 82.6(1), N2–C1–N1 106.1(5), N3–C28–N4 106.2(4).

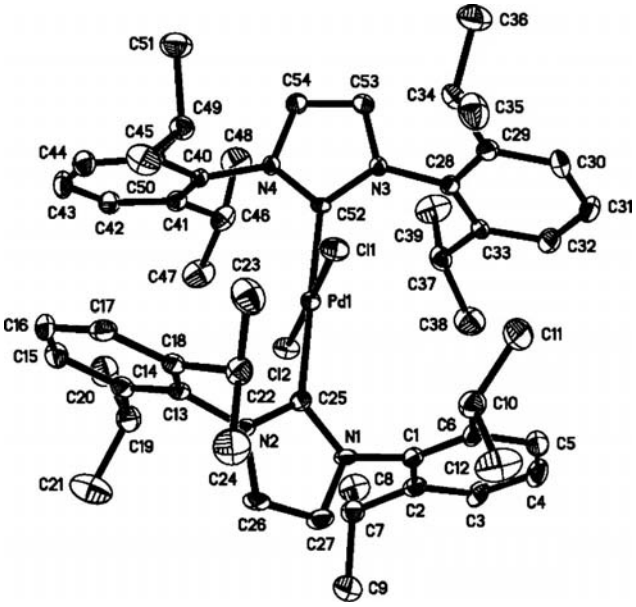

Figure 6. ORTEP drawing of **11**·Et_2O. Selected bond lengths [Å] and angles [°]: Pd1–C52 2.040(4), Pd1–C25 2.043(4), Pd1–Cl1 2.230(1), Pd1–Cl2 2.303(1), N1–C25 1.363(6), N2–C25 1.358(5), N3–C52 1.361(5), N4–C52 1.363(5); C52–Pd1–C25 179.1(2), C52–Pd1–Cl1 87.9(1), C25–Pd1–Cl1 91.2(1), C52–Pd1–Cl2 92.1(1), C25–Pd1–Cl2 88.8(1), Cl1–Pd1–Cl2 178.67(5).

phane–NHC–Pd^0 and bis(NHC)–Pd^0 complexes. To the best of our knowledge, our results provide the first case for the oxidative addition of small alkyl halides to NHC-stabilized Pd^0 complexes.

Under mild conditions, *p*-nitroiodobenzene readily undergoes oxidative addition to the bis(NHC)–Pd^0 complex stabilized by maleic anhydride.[11] In addition, Caddick and Cloke et al.[12] independently reported that the reaction of the bis(NHC)–Pd^0 complex (**4**) with aryl chloride does not produce a four-coordinate complex at room temperature or even under heating conditions, but an arylimidazolium compound, a reductive-elimination product, is produced. In contrast to the above-mentioned results, our bis(NHC)–Pd^0 complexes **3** and **4** smoothly underwent oxidative addition with organic halogenated solvents at room temperature (Scheme 5). In our case, a small steric requirement of organic reagents (dichloromethane and chloroform) seemed to be an important factor responsible for the observed oxidative addition reactivity. The molecular structures of **10** and **11** clearly demonstrate the steric congestion around the Pd metal, which may hinder organic halides from undergoing oxidative addition to NHC–Pd^0 compounds.

Reactivity of PMe_3–NHC–Pd^0 Complexes toward Organic Halides and a Chelated Phosphane

We further examined the reactivity of the PMe_3–NHC–Pd^0 complex toward other organic halides, including bromobenzene, *trans*-1,2-dichloroethylene, and 5,5′-dibromo-2,2′-bithiophene (Scheme 6 and Scheme 7). Reactions of **2** with excess amounts of bromobenzene and *trans*-1,2-dichloroethylene at room temperature proceeded to give the expected oxidative addition products, [(Me_3P)Pd(C_6H_5)Br(SIPr)] (**12**, 65% yield) or [(Me_3P)Pd(CH=CHCl)Cl(SIPr)] (**13**, 39% yield), respectively, which were characterized by spectroscopy and elemental analyses. Unfortunately, the similar reaction with *cis*-ClCH=CHCl could not give pure products on account of its thermal instability in solution. Grusin and co-workers[50] previously prepared a similar Pd–(aryl) complex from IPr·HCl and [($Ph_3P)_2$-$Pd_2Ph_2(\mu\text{-}OH)_2$].

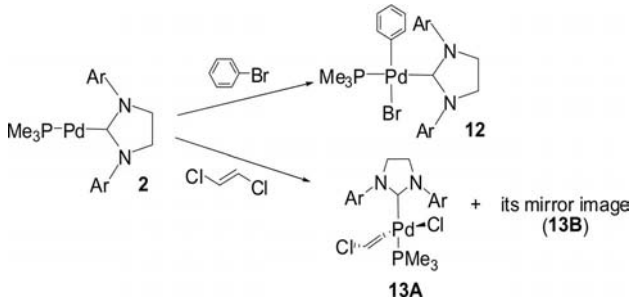

Scheme 6.

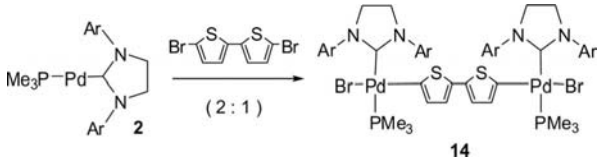

Scheme 7.

A molecular structure of complexes **12** is presented in Figure 7. The coordination sphere Pd1 can be described as a square plane, and the Br and phenyl ligands are mutually *trans*. The molecular plane (P1, Br1, C1, C28, Pd1) is roughly planar with an average atomic displacement of 0.065(1) Å, and the phenyl ligands are essentially perpendicular to this plane with the dihedral angle of 84.78(7)°.

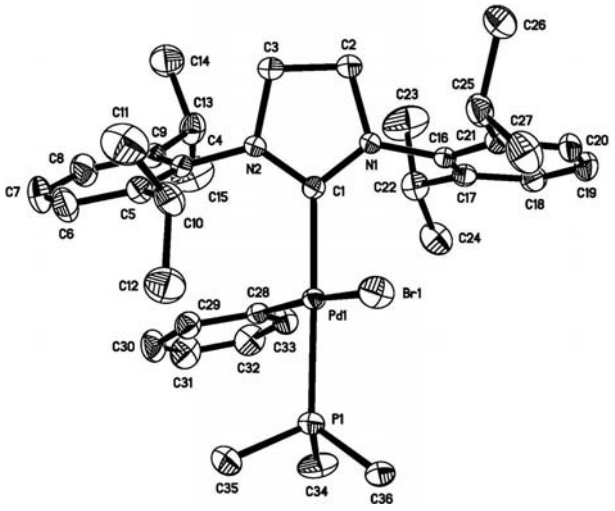

Figure 7. ORTEP drawing of **12**. Selected bond lengths [Å] and angles [°]: Pd1–C28 2.022(3), Pd1–C1 2.074(3), Pd1–P1 2.3185(8), Pd1–Br1 2.5178(4), N1–C1 1.351(3), N1–C16 1.445(3), N1–C2 1.480(3), N2–C1 1.342(3), N2–C4 1.433(3), N2–C3 1.473(3), C2–C3 1.488(4); C28–Pd1–C1 97.65(10), C28–Pd1–P1 82.95(8); C1–Pd1–P1 178.06(8), C28–Pd1–Br1 170.36(8).

The molecular structure of **13** in Figure 8 clearly reveals that *trans*-ClCH=CHCl undergoes C–Cl *trans* addition to the PMe_3–NHC–Pd^0 complex. The oxidative addition of C–Cl bond of *trans*-1,2-dichloroethylene above and below the molecular plane of the PMe_3–NHC–Pd^0 compound might have led to the formation of enantiomers (**13A** and **13B**). The ORTEP drawing of **13** exhibits an enantiomeric pair. The enantiomers **13A** (Figure 8, A) and **13B** (Figure 8, B) have practically the same bond lengths and angles, and have the NHC ligand *trans* to the PMe_3 ligand. The molecular plane in both enantiomers, defined by two C, one P, one Cl, and one Pd atoms, is essentially planar [the average atomic displacement is 0.0151(2) or 0.010(2) Å]. The carbene carbon atom (N*C*N) of the imidazoline ring appears as a doublet ($J_{P,C}$ = 194 Hz) at δ = 201.9 ppm in the ^{13}C NMR spectra.

Scheme 7 shows the oxidative addition of the C–Br bond of 5,5′-dibromo-2,2′-bithiophene to two Pd centers of complex **2** to give a dinuclear Pd^{II} complex (**14**) with a bridging bithiophene group. The two singlets assignable to the C*H* protons on the bridging thiophene rings spectra are observed at δ = 5.22 and 6.38 ppm in the ^1H NMR spectra of complex **14**. In particular, the methine signals C*H*$(CH_3)_2$ of the 2,6-diisopropylphenyl groups appear as a normal septet (J = 6.4 Hz) at δ = 3.74 ppm and a broad signal at δ = 3.42 ppm, strongly indicating the free rotation of one imidazoline moiety. In spite of several attempts to improve the

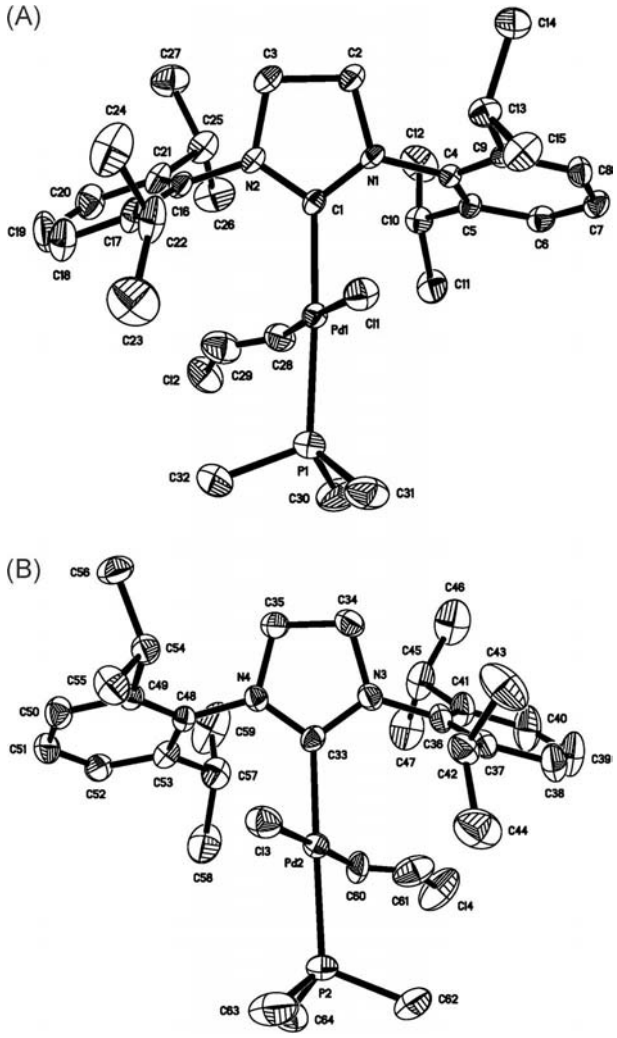

Figure 8. (A) ORTEP drawing of enantiomer A of complex **13**. (B) ORTEP drawing of enantiomer B of complex **13**. Selected bond lengths [Å] and angles [°]: Pd1–C28 2.014(6), Pd1–C1 2.041(4), Pd1–P1 2.296(2), Pd1–Cl1 2.373(1), Pd2–C60 2.077(5), Pd2–C33 2.047(4), Pd2–P2 2.292(1), Pd2–Cl3 2.353(1), N1–C1 1.351(5), N1–C2 1.468(5), N2–C1 1.342(5), N2–C3 1.451(5), N4–C33 1.349(5), N4–C48 1.441(5), N4–C35 1.471(5), N3–C33 1.353(5), N3–C36 1.444(5), N3–C34 1.462(5); C1–Pd1–P1 177.2(1), C28–Pd1–Cl1 176.5(2), C33–Pd2–P2 179.0(1), C60–Pd2–Cl3 176.7(2), N1–C1–N2 106.5(4), N4–C33–N3 106.3(4).

crystal quality for X-ray diffraction analysis, we obtained very thin plate-shaped crystals. As a result, the number of reflections with $I > 2\sigma(I)$ is small, and therefore the ratio of the number of reflections to the number of parameters is rather low (3505:373 in Table 1). However, the obtained molecular structure of **14** shows a definite atom–atom connectivity to clearly confirm its 3D structure (Figure 9).

We also attempted the ligand replacement of PMe_3–NHC–Pd^0 complex **1** with a chelating phosphane [dppp = 1,3-bis(diphenylphosphanyl)propane], as shown in Scheme 8.

This reaction proceeds smoothly to produce the bis(dppp)–Pd^0 compound, [Pd(dppp)$_2$], in 69% yield, which was characterized by elemental analysis, NMR spec-

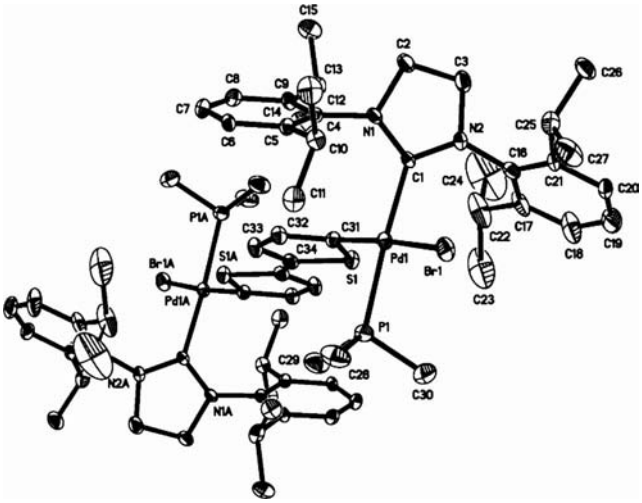

Figure 9. ORTEP drawing of complex **14**·C_6H_{14}. Unlabeled atoms are related to labeled ones by inversion. The co-crystallized hexane molecule is omitted for clarity. Selected bond lengths [Å] and angles [°]: Pd1–C31 2.017(5), Pd1–C1 2.077(6), Pd1–P1 2.299(2), Pd1–Br1 2.4983(8), N1–C11.341(7), N1–C2 1.496(7), N2–C1 1.330(7), N2–C3 1.474(8); C31–Pd1–C1 95.2(2), C31–Pd1–P1 87.4(2), C1–Pd1–P1 176.5(2), C31–Pd1–Br1 172.1(2), C1–Pd1–Br1 90.8(1), N2–C1–N1108.1(6).

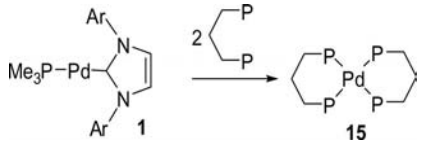

Scheme 8.

troscopy, and X-ray diffraction. The molecular structure of **15** (Figure 10) shows an extremely distorted tetrahedral structure. This reaction may reflect the higher lability of the

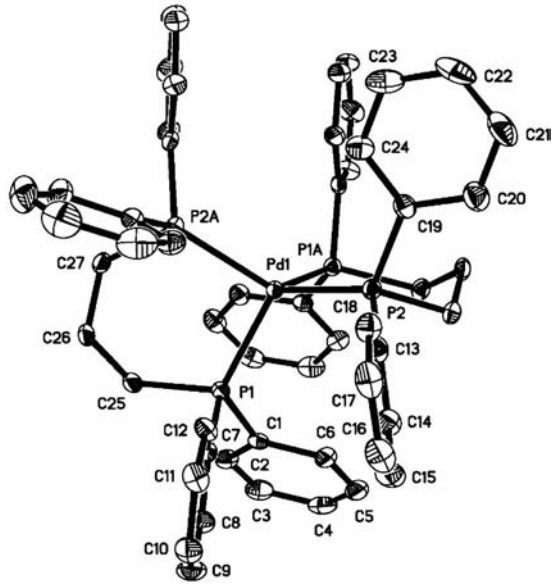

Figure 10. ORTEP drawing of **15**. Selected bond lengths [Å] and angles [°]: Pd1–P2 2.3239(7), Pd1–P1 2.3269(7); P2–Pd1–P2#1 121.62(4), P2–Pd1–P1#1 97.74(3).

PMe_3 and NHC ligands compared to the dppp ligand, which is expected to have chelating effects.

Conclusion

In summary, novel heteroleptic PMe_3–NHC–Pd^0 complexes were prepared from a diethyl Pd^{II} compound, and then homoleptic bis(NHC)–Pd^0 complexes were prepared by treating PMe_3–NHC–Pd^0 complexes with one additional equivalent of NHC. Oxidative additions of various organic halides to these NHC complexes were investigated. In particular, we observed the facile oxidative addition of small alkyl halides such as dichloromethane and chloroform to these NHC–Pd^0 complexes. Complex **6**, [(Me_3P)ClPd(CH=CHCl)(SIPr)], exhibits enantiomerism.

Experimental Section

General: All manipulations of air-sensitive complexes were performed under N_2 or Ar by standard Schlenk-line techniques. Solvents were distilled from Na–benzophenone. The analytical laboratories at Kangnung-Wonju National University carried out elemental analyses with a CE instruments EA1110. IR spectra were recorded with a Perkin–Elmer BX spectrophotometer. NMR (^{1}H, ^{13}C{^{1}H}, and ^{31}P{^{1}H}) spectra were obtained with a JEOL Lamda 300 and ECA 600 MHz spectrometer. Chemical shifts were referenced to internal Me_4Si or to external 85% H_3PO_4. Some of the X-ray analysis was carried out at the Jeonju Center at the Basic Science Institute of Korea. *trans*-[$PdEt_2(PMe_3)_2$] was prepared by the literature method.[16b] IPr [1,3-bis(2,6-diisopropylphenyl)imidazol-2-ylidene] and SIPr [1,3-bis(2,6-diisopropylphenyl)-4,5-dihydroimidazol-2-ylidene] were prepared by the literature method[51] or purchased from Strem Chemical.

Preparations

[(Me_3P)Pd(IPr)] (1) and [(Me_3P)Pd(SIPr)] (2): Styrene (0.604 g, 5.81 mmol) and THF (3 mL) were added sequentially to a Schlenk flask that contained *trans*-[$PdEt_2(PMe_3)_2$] (0.736 g, 2.32 mmol) at 0 °C. The mixture was heated at 55 °C for 1 h to give a yellow solution. At room temperature, IPr (0.885 g, 2.28 mmol) was added to the mixture, and then the initial colorless solution turned to an orange solution. After stirring the reaction mixture for 3 h, the solvent was removed completely under vacuum, and then the resulting oily residue was solidified with hexane. The solids were filtered and washed with hexane (2 mL × 3) to give pale yellow solids of **1** (0.852 g, 65%). ^{1}H NMR (600 MHz, C_6D_6, 10 °C): δ = 0.68 [br., 9 H, P(CH_3)$_3$], 1.12 [d, J = 6.8 Hz, 12 H, CH(CH_3)$_2$], 1.46 [br., 12 H, CH(CH_3)$_2$], 3.21 [br., 4 H, CH(CH$_3$)$_2$], 6.63 (br., 2 H, CH), 6.90–6.97 (m, 2 H, Ar–H), 7.05–7.10 (m, 2 H, Ar–H), 7.14–7.19 (m, 2 H, Ar–H), 7.22–7.29 (m, 2 H, Ar–H) ppm. ^{13}C{^{1}H} NMR (151 MHz, [D_6]acetone, –40 °C): δ = 17.9 [d, $J_{P,C}$ = 29 Hz, P(CH_3)$_3$], 26.6, 26.9, 29.9, 30.0 [s, CH(CH_3)$_2$], 69.5 [s, CH(CH$_3$)$_2$], 107.6 (d, $J_{P,C}$ = 6.9 Hz, NCH=), 127.5, 128.5, 133.8, 139.7, 148.1, 152.4 (s, Ar–C), 178.5 (d, $J_{P,C}$ = 16 Hz, NCN) ppm. ^{31}P{^{1}H} NMR (243 MHz, C_6D_6, 10 °C): δ = –28.6 (s) ppm.

Complex **2** (84%) was prepared in a similar way. ^{1}H NMR (600 MHz, C_6D_6, 10 °C): δ = 0.67 [d, J = 4.1 Hz, 9 H, P(CH_3)$_3$], 1.25 [d, J = 6.8 Hz, 12 H, CH(CH_3)$_2$], 1.60 [br., 12 H, CH(CH_3)$_2$], 3.42 [br., 8 H, CH_2, CH(CH$_3$)$_2$], 6.96–7.22 (m, 6 H, aromatic) ppm. ^{13}C{^{1}H} NMR (151 MHz, C_6D_6, 10 °C): δ = 19.2 [d, $J_{P,C}$ = 14 Hz,

P(CH_3)$_3$], 24.9, 28.6 [s, CH(CH_3)$_2$], 53.1 [s, CH(CH$_3$)$_2$], 123.8, 125.4, 138.4, 147.1 (s, Ar–*C*) . The ^{13}C signal due to the N*C*N for **2** could not be assigned due to the broadness. ^{31}P{^{1}H} NMR (243 MHz, C_6D_6 at 10 °C): δ = –28.8 (s) ppm.

[Pd(IRr)$_2$] (3) and [Pd(SIPr)$_2$] (4): At room temperature, a solution of IPr (0.417 g, 1.05 mmol) in toluene (7 mL) was added to a solution of [(Me$_3$P)Pd(IPr)] (0.547 g, 0.96 mmol) in toluene (5 mL). The initial pale yellow solution slowly turned into an orange solution. After stirring for 3 h at room temperature, the solvent was completely removed under vacuum, and then the resulting oily residue was solidified with hexane. The solids were filtered and washed with hexane (2 mL × 3) to give yellow solids. Recrystallization from toluene gave yellow crystals of **3** (0.541 g, 64%). $C_{54}H_{72}N_4Pd$ (883.60): calcd. C 73.40, H 8.21, N 6.34; found C 73.52, H 8.73, N 6.24. ^{1}H NMR (600 MHz, C_6D_6, 23 °C): δ = 1.11 [d, *J* = 6.0 Hz, 24 H, CH(CH_3)$_3$], 1.20 [d, *J* = 6.0 Hz, 24 H, CH(CH_3)$_2$], 2.88 [sept, *J* = 6.0 Hz, 8 H, C*H*(CH$_3$)$_2$], 6.27 (s, 4 H, CH), 7.09 (d, *J* = 9.0 Hz, 8 H, Ar–*H*), 7.29 (t, *J* = 9.0 Hz, 4 H, Ar–*H*) ppm. ^{13}C{^{1}H} NMR (151 MHz, C_6D_6, 23 °C): δ = 24.0, 25.1, 28.7 [s, CH(*C*H$_3$)$_2$], 121.2, 123.4, 128.6, 139.1, 146.0 (s, Ar–*C*), 198.8 (s, N*C*N) ppm.

Complex **4** (46%) was prepared analogously. The analytical data for **4** are identical to those in literature.[18]

Complexes **3** and **4** were previously prepared from [Pd{P(*o*-tolyl)$_3$}$_2$] with IPr or SIPr by the groups of Caddick, Cloke,[18] and Herrmann.[19]

***trans*-[Pd(PMe$_3$)Et$_2$(IPr)] (5) and *trans*-[Pd(PMe$_3$)Et$_2$(SIPr)] (6):** IPr (0.434 g, 1.12 mmol) solution dissolved in THF (4 mL) was added to a Schlenk flask that contained *trans*-[PdEt$_2$(PMe$_3$)$_2$] (0.354 g, 1.12 mmol) at 0 °C. After stirring the reaction mixture overnight at room temperature, the solvent was completely removed under vacuum. A dithyl ether/*n*-hexane mixture (3:1) was added to the resulting oily residue, and then it was stored in the freezer to give crude solids. The solids were filtered, washed with hexane (2 mL × 2), and recrystallized from dithyl ether to give white crystals of **5** (171 g, 24%). $C_{34}H_{55}N_2PPd$ (629.21): calcd. C 64.90, H 8.81, N 4.45; found C 64.83, H 9.32, N 4.38. ^{1}H NMR (600 MHz, [D$_6$]acetone, –40 °C): δ = –0.11 (dq, *J* = 7.3 Hz, 4 H, Pd–CH_2), 0.40 (dt, *J* = 2.3, 7.8 Hz, 6 H, Pd–CH$_2$CH_3), 1.07 [d, *J* = 7.8 Hz, 9 H, P(CH_3)$_3$], 1.11 [d, *J* = 6.8 Hz, 12 H, CH(CH_3)$_2$], 1.32 [d, *J* = 6.9 Hz, 12 H, CH(CH_3)$_2$], 3.31 [sept, *J* = 6.8 Hz, 4 H, C*H*(CH$_3$)$_2$], 7.30 (d, *J* = 7.8 Hz, 4 H, Ar–*H*), 7.40 (t, *J* = 7.8 Hz, 2 H, Ar–*H*), 7.48 (s, 2 H, CH=) ppm. ^{13}C{^{1}H} NMR (151 MHz, [D$_6$]acetone, –40 °C): δ = 3.45 (d, $J_{P,C}$ = 10 Hz, Pd–*C*H$_2$), 14.7 [d, $J_{P,C}$ = 24 Hz, P(*C*H$_3$)$_3$], 17.4 (d, $J_{P,C}$ = 3.5 Hz, CH$_2$*C*H$_3$), 23.1 [s, CH(*C*H$_3$)$_2$], 25.9 [s, CH(*C*H$_3$)$_2$], 29.7 [s, *C*H(CH$_3$)$_2$], 122.9 (N*C*H=), 124.3, 129.5, 137.9, 146.1 (s, Ar–*C*), 196.0 (d, $J_{P,C}$ = 154 Hz, N*C*N) ppm. ^{31}P{^{1}H} NMR (243 MHz, [D$_6$]acetone, –40 °C): δ = –11.7 (s) ppm.

Complex **6** (33%) was prepared analogously. $C_{34}H_{57}N_2PPd$ (631.22): calcd. C 64.69, H 9.10, N 4.44; found C 64.35, H 9.66, N 4.26. ^{1}H NMR (600 MHz, [D$_6$]acetone, –40 °C): δ = –0.03 (dq, *J* = 7.3 Hz, 4 H, Pd–CH_2), 0.35 (dt, *J* = 2.3, 7.3 Hz, 6 H, Pd–CH$_2$CH_3), 1.04 [d, *J* = 7.3 Hz, 9 H, P(CH_3)$_3$], 1.23 [d, *J* = 6.8 Hz, 12 H, CH(CH_3)$_2$], 1.37 [d, *J* = 6.9 Hz, 12 H, CH(CH_3)$_2$], 3.59 [sept, *J* = 6.9 Hz, 4 H, C*H*(CH$_3$)$_2$], 4.00 (s, 4 H, NCH_2), 7.24 (d, *J* = 7.3 Hz, 4 H, Ar–*H*), 7.30 (t, *J* = 7.5 Hz, 2 H, Ar–*H*) ppm. ^{13}C{^{1}H} NMR (151 MHz, [D$_6$]acetone, –40 °C): δ = 2.18 (d, $J_{P,C}$ = 10 Hz, Pd–*C*H$_2$), 14.0 [d, $J_{P,C}$ = 23 Hz, P(*C*H$_3$)$_3$], 16.8 (d, $J_{P,C}$ = 3.5 Hz, Pd–CH$_2$*C*H$_3$), 23.4 [s, CH(*C*H$_3$)$_2$], 26.1 [s, CH(*C*H$_3$)$_2$], 28.4 [s, *C*H(CH$_3$)$_2$], 54.1 (d, $J_{P,C}$ = 5.2 Hz, N*C*H$_2$), 124.0, 127.5, 137.8, 146.6 (s, Ar–*C*), 220.8 (d, $J_{P,C}$ = 146 Hz, N*C*N) ppm. ^{31}P{^{1}H} NMR (243 MHz, [D$_6$]acetone, –40 °C): δ = –12.3 (s) ppm.

Reactivity of [(Me$_3$P)Pd(IPr)], [(Me$_3$P)Pd(SIPr)], [Pd(IPr)$_2$], and [Pd(SIPr)$_2$] toward Organic Halides (Dichloromethane, Chloroform, Bromobenzene, *trans*-1,2-Dichloroethylene, 5,5′-Dibromo-2,2′-bithiophene) and dppp

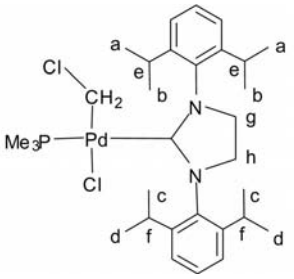

[(Me$_3$P)ClPd(CH$_2$Cl)(IPr)] (7), [(Me$_3$P)ClPd(CH$_2$Cl)(SIPr)] (8), [ClPd(CH$_2$Cl)(IPr)$_2$] (9), and [ClPd(CH$_2$Cl)(SIPr)$_2$] (10): Complex **1** (0.460 g, 0.81 mmol) was dissolved in CH_2Cl_2 (3 mL). After stirring for 3 h at room temperature, the solvent was completely removed under vacuum, and then the resulting oily residue was solidified with hexane. The solids were filtered and dried to give gray solids of crude products. The final products were recrystallized from a diethyl ether/hexane mixture to give final product **7** (0.443 g, 84%). $C_{31}H_{47}Cl_2N_2PPd$ (656.02): calcd. C 56.76, H 7.22, N 4.27; found C 56.72, H 7.83, N 4.12. ^{1}H NMR (600 MHz, $CDCl_3$, –40 °C): δ = 1.12 [d, *J* = 6.9 Hz, 6 H, CH(CH_{3c})$_2$], 1.15 [d, *J* = 6.9 Hz, 6 H, CH(CH_{3a})$_2$], 1.20 [d, *J* = 9.7 Hz, 9 H, P(CH_3)$_3$], 1.36 [d, *J* = 6.9 Hz, 6 H, CH(CH_{3b})$_2$], 1.47 [d, *J* = 6.4 Hz, 6 H, CH(CH_{3d})$_2$], 2.79 [sept, *J* = 6.8 Hz, 2 H, C*H*(CH$_3$)$_{2e}$], 3.08 (d, *J* = 7.3 Hz, 2 H, CH_2), 3.26 [sept, *J* = 6.8 Hz, 2 H, C*H*(CH$_3$)$_{2f}$], 7.15 (s, 2 H, CH=), 7.30 (d, *J* = 7.8 Hz, 2 H, Ar-*H*), 7.36 (d, *J* = 7.8 Hz, 2 H, Ar–*H*), 7.48 (t, *J* = 7.8 Hz, 2 H, Ar–*H*) ppm. ^{13}C{^{1}H} NMR (151 MHz, $CDCl_3$, –40 °C): δ = 12.9 [d, $J_{P,C}$ = 28 Hz, P(*C*H$_3$)$_3$], 23.0 [s, CH(*C*$_b$H$_3$)$_2$], 23.8 [s, CH(*C*$_d$H$_3$)$_2$], 26.4 [s, CH(*C*$_{c+a}$H$_3$)$_2$], 28.8 [s, *C*$_f$H(CH$_{3c}$)$_2$], 28.9 [s, *C*$_e$H(CH$_{3c}$)$_2$], 29.3 (s, CH$_2$), 123.7 (s, N–*C*H), 123.8, 123.9 (s, N–*C*H=), 124.5, 129.7, 135.5, 144.5, 146.9 (s, Ar–*C*), 183.6 (d, $J_{P,C}$ = 158 Hz, N*C*N) ppm. ^{31}P{^{1}H} NMR (243 MHz in $CDCl_3$, –40 °C): δ = –12.7 (s) ppm.

Complex **8** (69%) was prepared analogously. $C_{32}H_{49}Cl_2N_2PPd$ (670.04): calcd. C 56.58, H 7.51, N 4.26; found C 56.54, H 8.19, N 4.06. ^{1}H NMR (600 MHz, $CDCl_3$, –40 °C): δ = 1.15 [d, *J* = 9.7 Hz, 9 H, P(CH_3)$_3$], 1.26 [d, *J* = 6.8 Hz, 6 H, CH(CH_{3c})$_2$], 1.30 [d, *J* = 6.4 Hz, 6 H, CH(CH_{3a})$_2$], 1.40 [d, *J* = 6.8 Hz, 6 H, CH(CH_{3b})$_2$], 1.53 [d, *J* = 6.8 Hz, 6 H, CH(CH_{3d})$_2$], 3.14 (d, *J* = 7.3 Hz, 2 H, CH_2), 3.16 [sept, *J* = 6.8 Hz, 2 H, C*H*(CH$_3$)$_{2e}$], 3.61 [sept, *J* = 6.8 Hz, 2 H, C*H*(CH$_3$)$_{2f}$], 3.95 (m, 2 H, NCH_{2g}), 4.03 (m, 2 H, NCH_{2h}), 7.25 (dd, *J* = 1.4, 7.7 Hz, 2 H, Ar–*H*), 7.32 (dd, *J* = 1.4, 7.7 Hz, 2 H, Ar–*H*), 7.40 (t, *J* = 7.8 Hz, 2 H, Ar–*H*) ppm. ^{13}C{^{1}H} NMR (151 MHz, $CDCl_3$, –40 °C): δ = 12.5 [d, $J_{P,C}$ = 28 Hz, P(*C*H$_3$)$_3$], 23.4 [s, CH(*C*$_b$H$_3$)$_2$], 24.3 [s, CH(*C*$_d$H$_3$)$_2$], 26.7 [s, CH(*C*$_c$H$_3$)$_2$], 26.8 [s, CH(*C*$_a$H$_3$)$_2$], 28.4 [s, *C*$_f$H(CH$_{3c}$)$_2$], 28.6 [s, *C*$_e$H(CH$_{3c}$)$_2$], 29.2 (s, CH$_2$), 53.8 (s, N–*C*H$_2$), 53.9 (s, N–*C*H$_2$), 123.8, 124.6, 128.5, 135.5, 145.3, 147.7 (s, Ar–*H*), 209.8 (d, $J_{P,C}$ = 147 Hz, N*C*N) ppm. ^{31}P{^{1}H} NMR (243 MHz, $CDCl_3$, –40 °C): δ = –12.7 (s) ppm.

Complex **3** (0.177 g, 0.20 mmol) was dissolved in CH_2Cl_2 (3 mL). The initial orange mixture turned colorless. After stirring for 3 h at room temperature, the solvent was completely removed under vacuum, and then the resulting solids were crystallized from diethyl ether to give final product **9** (0.183 g, 94%). $C_{55}H_{74}Cl_2N_4Pd$

(968.53): calcd. C 68.21, H 7.70, N 5.78; found C 68.57, H 7.99, N 5.32. ^{1}H NMR (600 MHz, CD_2Cl_2, –40 °C): δ = 0.83 [d, J = 6.9 Hz, 12 H, CH(CH_3)$_2$], 0.89 [d, J = 7.3 Hz, 12 H, CH(CH_3)$_2$], 0.90 [d, J = 7.3 Hz, 12 H, CH(CH_3)$_2$], 0.96 [d, J = 6.9 Hz, 12 H, CH(CH_3)$_2$], 2.66 [sept, J = 6.8 Hz, 4 H, CH(CH$_3$)$_2$], 3.04 [sept, J = 6.8 Hz, 4 H, CH(CH$_3$)$_2$], 3.05 (s, 2 H, CH_2), 6.83 (s, 4 H, CH=), 7.11, 7.13, 7.14, 7.15 (br., 8 H, Ar–H), 7.37 (t, J = 7.8 Hz, 4 H, Ar–H) ppm. ^{13}C{^{1}H} NMR (151 MHz, CD_2Cl_2, –40 °C): δ = 22.5 [s, CH(CH_3)$_2$], 22.6 [s, CH(CH_3)$_2$], 26.2 [s, CH(CH_3)$_2$], 26.4 [s, CH(CH_3)$_2$], 28.1 [s, CH(CH$_3$)$_2$], 28.1 [s, CH(CH$_3$)$_2$], 28.5 (s, CH_2), 123.4 (s, N–CH=), 123.5 (s, N–CH=), 124.1, 124.9, 124.2, 129.2, 129.3, 136.7, 145.3, 147.2 (s, Ar–C), 182.8 (s, NCN) ppm.

Complex **4** analogously produced **10** (53%). $C_{55}H_{78}Cl_2N_4Pd$ (972.56): calcd. C 67.92, H 8.08, N 5.76; found C 67.83, H 8.47, N 5.73. ^{1}H NMR (600 MHz, $CDCl_3$, –30 °C): δ = 0.92 [d, J = 6.9 Hz, 12 H, CH(CH_3)$_2$], 0.97 [d, J = 6.4 Hz, 12 H, CH(CH_3)$_2$], 1.00 [d, J = 6.9 Hz, 12 H, CH(CH_3)$_2$], 1.08 [d, J = 6.4 Hz, 12 H, CH(CH_3)$_2$], 3.07 (s, 2 H, CH_2), 3.08 [sept, J = 6.4 Hz, 4 H, CH(CH$_3$)$_2$], 3.40 [sept, J = 6.9 Hz, 4 H, CH(CH$_3$)$_2$], 3.70 (m, 8 H, NCH_2), 7.06, 7.07, 7.08, 7.09 (br., 8 H, Ar–H), 7.27 (t, J = 7.3 Hz, 4 H, Ar–H) ppm. ^{13}C{^{1}H} NMR (151 MHz, $CDCl_3$, –30 °C): δ = 23.4 [s, CH(CH_3)$_2$], 23.9 [s, CH(CH_3)$_2$], 26.8 [s, CH(CH_3)$_2$], 27.0 [s, CH(CH_3)$_2$], 28.2 [s, CH(CH$_3$)$_2$], 28.6 [s, CH(CH$_3$)$_2$], 29.2 (s, CH_2), 54.0 (s, N–CH_2), 124.0, 124.9, 128.4, 137.4, 146.2, 148.2 (s, Ar–C), 209.0 (s, NCN) ppm.

[Pd(IPr)$_2$Cl$_2$] (11): Complex **3** (0.152 g, 0.17 mmol) was dissolved in $CHCl_3$ (3 mL). The initial yellow mixture turned colorless. After stirring for 3 h, the solvent was completely removed under vacuum, and then the resulting solids were crystallized from a diethyl ether to give white crystals of **11** (0.137 g, 79%). ^{1}H NMR (600 MHz, CD_2Cl_2, –40 °C): δ = 0.89 [d, J = 6.9 Hz, 24 H, CH(CH_3)$_2$], 0.93 [d, J = 6.8 Hz, 24 H, CH(CH_3)$_2$], 2.86 [sept, J = 6.8 Hz, 8 H, CH(CH$_3$)$_2$], 6.83 (s, 4 H, NCH=), 7.12 (d, J = 7.7 Hz, 8 H, Ar–H), 7.42 (t, J = 7.8 Hz, 4 H, Ar–H) ppm. ^{13}C{^{1}H} NMR (151 MHz, CD_2Cl_2, –40 °C): δ = 22.7 [s, CH(CH_3)$_2$], 26.0 [s, CH(CH_3)$_2$], 28.2 [s, CH(CH_3)$_2$], 123.8 (s, N–CH=), 124.3, 129.4, 136.7, 146.2 (s, Ar–C), 171.7 (s, NCN) ppm. $C_{54}H_{72}Cl_2N_4Pd$ (954.50): calcd. C 67.95, H 7.60, N 5.87; found C 68.10, H 8.12, N 5.82.

[(Me$_3$P)BrPd(C$_6$H$_5$)(SIPr)] (12): Bromobenzene (0.095 g, 0.60 mmol) and THF (2 mL) were sequentially added to a Schlenk flask that contained **2** (0.230 g, 0.40 mmol) at room temperature. After stirring for 3 h at room temperature, the solvent was completely removed under vacuum, and then the resulting oily residue was solidified with hexane. The solids were filtered and washed with hexane (2 mL × 3) to give yellow solids of **12** (0.189 g, 65%). $C_{36}H_{52}BrN_2PPd$ (730.11): calcd. C 59.22, H 7.18, N 3.84; found C 59.57, H 7.50, N 3.74. ^{1}H NMR (600 MHz, $CDCl_3$, 23 °C): δ = 0.75 [d, J = 9.7 Hz, 9 H, P(CH_3)$_3$], 0.80 [d, J = 6.4 Hz, 6 H, CH(CH_3)$_{3c}$], 1.07 [d, J = 6.4 Hz, 6 H, CH(CH_3)$_{3a}$], 1.25 [d, J = 6.4 Hz, 6 H, CH(CH_3)$_{3b}$], 1.58 [d, J = 6.4 Hz, 6 H, CH(CH_3)$_{3d}$], 3.12 [sept, J = 6.4 Hz, 2 H, CH(CH$_3$)$_{2e}$], 4.03 [sept, J = 6.4 Hz, 2 H, CH(CH$_3$)$_{2f}$], 3.88–3.91 (m, 2 H, NCH_2), 4.09–4.12 (m, 2 H, NCH_2), 6.19 (m, 2 H, Ar–H), 6.56 (m, 3 H, Ar–H), 7.13 (d, J = 7.8 Hz, 2 H, Ar–H), 7.35 (d, J = 6.0 Hz, 2 H, Ar–H), 7.39 (t, J = 7.8 Hz, 2 H, Ar–H) ppm. ^{13}C{^{1}H} NMR (75 MHz, $CDCl_3$, 23 °C): δ = 14.0 [d, $J_{P,C}$ = 28 Hz, P(CH_3)$_3$], 22.6 [s, CH(C$_b$H$_3$)$_2$], 25.1 [s, CH(C$_d$H$_3$)$_2$], 26.4 [s, CH(C$_c$H$_3$)$_2$], 26.9 [s, CH(C$_a$H$_3$)$_2$], 28.4 [s, C$_f$H(CH$_{3c}$)$_2$], 28.7 [s, C$_e$H(CH$_{3c}$)$_2$], 53.8 (s, N–CH_2), 53.9 (s, N–CH_2), 121.5, 123.7, 124.8, 126.6, 128.5, 137.7 (t, $J_{P,C}$ = 4.5 Hz), 146.5, 148.5, 152.1 (s, Ar–C), 210.3 (d, $J_{P,C}$ = 149 Hz, NCN) ppm. ^{31}P{^{1}H} NMR (243 MHz, $CDCl_3$, 23 °C): δ = –14.8 (s) ppm.

[(Me$_3$P)ClPd(CH=CHCl)(SIPr)] (13): *trans*-Dichloroethylene (0.548 g, 5.7 mmol) and THF (4 mL) were sequentially added to a Schlenk flask that contained **2** (0.325 g, 0.57 mmol) at room temperature. After stirring for 3 h at room temperature, the solvent was completely removed under vacuum, and then the resulting residue was extracted with an excess amount of *n*-hexane. The collected filtrates were stored in the freezer to give white solids and then recrystallized from *n*-hexane to give white crystals of **13** (0.149 g, 39%). $C_{32}H_{49}Cl_2N_2PPd$ (670.04): calcd. C 57.36, H 7.37, N 4.18; found C 57.47, H 7.80, N 3.94. ^{1}H NMR (600 MHz, $CDCl_3$ at –40 °C): δ = 1.05 [d, J = 11 Hz, 9 H, P(CH_3)$_3$], 1.23 [d, J = 6.8 Hz, 12 H, CH(CH_3)$_3$], 1.48 [d, J = 6.4 Hz, 12 H, CH(CH_3)$_3$], 3.22 [sept, J = 7.0 Hz, 2 H, CH(CH$_3$)$_2$], 3.65 [sept, J = 7.0 Hz, 2 H, CH(CH$_3$)$_2$], 3.81 (d, J = 14 Hz, Pd–CH=CH), 3.90 (s, 2 H, NCH_2), 4.09 (s, 2 H, NCH_2), 5.74 (dd, J = 5.5, 14 Hz, Pd–CH=CH), 7.25 (d, J = 7.8 Hz, 4 H, Ar–H), 7.37 (t, J = 7.8 Hz, 2 H, Ar-H) ppm. ^{13}C{^{1}H} NMR (151 MHz in $CDCl_3$ at –40 °C): δ = 13.1 [d, $J_{P,C}$ = 29 Hz, P(CH_3)$_3$], 23.2, 24.3, 26.7, 28.4 [s, CH(CH_3)$_2$], 54.0 (s, NCH_2), 104.1 (t, $J_{P,C}$ = 10 Hz, Pd–CH), 123.8, 128.4, 136.0, 145.9 (s, Ar–C), 207.5 (d, $J_{P,C}$ = 156 Hz, NCN) ppm. ^{31}P{^{1}H} NMR (243 MHz in $CDCl_3$ at –40 °C): δ = –12.6 (s) ppm.

[{(Me$_3$P)(SIPr)BrPd}$_2$(μ-C$_4$H$_2$S–C$_4$H$_2$S)] (14): 5,5′-Dibromo-2,2′-bithiophene (0.066 g, 0.20 mmol) and THF (4 mL) were sequentially added to a Schlenk flask that contained **1** (0.239 g, 0.42 mmol) at room temperature. The initial insoluble material slowly dissolved to give a yellow solution. After stirring for 3 h at room temperature, the solvent was completely removed under vacuum, and then the resulting oily residue was solidified with hexane. The solids were filtered and washed with a diethyl ether (1 mL) to give yellow solids and recrystallized from an excess amount of diethyl ether to give yellow crystals of **14** (0.231 g, 77%). $C_{68}H_{98}Br_2N_4P_2Pd_2S_2$ (1470.26): calcd. C 55.55, H 6.72, N 3.81; found C 55.94, H 7.27, N 3.57. ^{1}H NMR (600 MHz, $CDCl_3$, 25 °C): δ = 0.89 [d, J = 9.6 Hz, 18 H, P(CH_3)$_3$], 1.07 [d, J = 5.9 Hz, 12 H, CH(CH_3)$_2$], 1.16 [d, J = 6.9 Hz,12 H, CH(CH_3)$_2$], 1.26 [d, J = 6.9 Hz,12 H, CH(CH_3)$_2$], 1.62 [d, J = 6.4 Hz, 12 H, CH(CH_3)$_2$], 3.42 [br., 4 H, CH(CH$_3$)$_2$], 3.74 [sept, J = 6.4 Hz, 4 H, CH(CH$_3$)$_2$], 3.90–3.96 (m, 8 H, NCH_2), 5.38 (d, J = 3.2 Hz, 2 H, SCH=), 6.42 (d, J = 3.2 Hz, 2 H, SCH=), 7.10 (d, J = 1.4 Hz, 2 H, Ar–H), 7.11 (d, J = 0.9 Hz, 2 H, Ar–H), 7.29 (d, J = 1.4 Hz, 2 H, Ar–H), 7.30 (d, J = 1.4 Hz, 2 H, Ar–H), 7.36 (d, J = 1.4 Hz, 2 H, Ar–H) ppm. ^{13}C{^{1}H} NMR (151 MHz, $CDCl_3$, –20 °C): δ = 13.4 [d, $J_{P,C}$ = 29 Hz, P(CH_3)$_3$], 23.2 [s, CH(CH_3)$_2$], 25.1 [s, CH(CH_3)$_2$], 26.7 [s, CH(CH_3)$_2$], 27.0 [s, CH(CH_3)$_2$], 28.6 [s, CH(CH$_3$)$_2$], 28.9 [s, CH(CH$_{3c}$)$_2$], 54.3 (NCH_2), 120.1, 122.0, 123.9,124.7, 128.6,129.5, 137.1, 138.4, 141.4, 146.3, 147.4 (s, Ar–H), 206.0 (d, $J_{P,C}$ = 165 Hz, NCN) ppm. ^{31}P{^{1}H} NMR (243 MHz, $CDCl_3$, –20 °C): δ = –12.1 (s) ppm.

[Pd(dppp)$_2$] (15): A solution of dppp in THF (0.220 g, 0.53 mmol) was added to a solution of **1** (0.304 g, 0.53 mmol) in THF (1 mL) at –40 °C. The reaction mixture was slowly warmed up to room temperature. After stirring the reaction mixture for 2 h, the yellow solids gradually precipitated. The resulting suspension was completely evaporated to give crude solids, which was washed with *n*-hexane and diethyl ether. The isolated solids were recrystallized from THF/*n*-hexane to give yellow crystals of **15** (0.171 g, 69%). $C_{54}H_{52}P_4Pd$ (931.30): calcd. C 69.64, H 5.62; found C 69.25, H 5.82. ^{1}H NMR (600 MHz, C_6D_6, 23 °C): δ = 1.42 (br., 4 H, –CH_2), 2.25 (br., 8 H, P–CH_2), 6.90–7.01 (m, 24 H, Ar–H), 7.50 (br., 16 H, Ar–H) ppm. ^{31}P{^{1}H} NMR (243 MHz, C_6D_6, 23 °C): δ = 4.46 (s) ppm.

Complex **15** was independently prepared from [Pd(C$_2$H$_4$)(dppp)] with dppp.[52]

X-ray Structure Determination: All X-ray data were collected with a Bruker Smart APEX or APEX2 diffractometer equipped with an Mo X-ray tube. Collected data were corrected for absorption with SADABS based upon the Laue symmetry by using equivalent reflections.[53] All calculations were carried out with SHELXTL programs.[54] All structures were solved by direct methods. All non-hydrogen atoms were refined anisotropically, and all hydrogen atoms were generated in ideal positions and refined in a riding model.

CCDC-802827 (for **6**), -802828 (for **7**), -802829 (for **8**), -802830 (for **10**), -802831 (for **11**·Et_2O), -802832 (for **12**), -802833 (for **13**), -802834 (for **14**·C_6H_{14}) and -802835 (for **15**) contain the supplementary crystallographic data for this paper. These data can be obtained free of charge from The Cambridge Crystallographic Data Centre via www.ccdc.cam.ac.uk/data_request/cif.

Acknowledgments

This work was supported by Basic Science Research Program through the National Research Foundation (NRF) of Korea funded by the Ministry of Education, Science, and Technology of Korea (grant number 2009-0074917)

[1] E. A. B. Kantchev, C. J. O'Brien, M. G. Organ, *Angew. Chem. Int. Ed.* **2007**, *46*, 2768–2813.
[2] a) N. Marion, S. P. Nolan, *Acc. Chem. Res.* **2008**, *41*, 1440–1449; S. P. Nolan (Ed.), *N-Heterocyclic Carbenes in Organic Synthesis*, Wiley-VCH, New York, **2006**; b) S. Diez-Gonzalez, S. P. Nolan, *Top. Organomet. Chem.* **2007**, *21*, 47–82.
[3] F. A. Glorious (Ed.), *N-Heterocyclic Carbenes in Transition Metal Catalysis*, Topics in Organometallic Chemistry, vol. 21, Springer-Verlag, Berlin/Heidelberg, Germany, **2007**.
[4] W. A. Herrmann, M. Elison, J. Fisher, C. Kocher, G. R. J. Artus, *Angew. Chem. Int. Ed. Engl.* **1995**, *34*, 2371–2374.
[5] G. Wilkinson, F. G. A. Sone, E. W. Abel, *Comprehensive Organometallic Chemistry*, Pergamon, Oxford, **1982**, vol. 6, pp. 243–260.
[6] N. Miyaura, A. Suzuki, *Chem. Rev.* **1995**, *95*, 2457–2483.
[7] I. P. Beletskaya, A. V. Cheprakov, *Chem. Rev.* **2000**, *100*, 3009–3066.
[8] J. K. Stille, *Angew. Chem. Int. Ed. Engl.* **1986**, *25*, 508–524.
[9] E. Negishi, *Handbook of Organopalladium Chemistry for Organic Synthesis*, John Wiley, **2002**, vol. I, p. 1051.
[10] C. M. Crudden, D. P. Allen, *Coord. Chem. Rev.* **2004**, *248*, 2247–2273.
[11] a) D. S. McGuinness, M. J. Green, K. J. Cavell, B. W. Skelton, A. H. White, *J. Organomet. Chem.* **1998**, *565*, 165–178; b) D. S. McGuinness, K. J. Cavell, B. W. Skelton, A. H. White, *Organometallics* **1999**, *18*, 1596–1605.
[12] a) S. Caddick, F. G. N. Cloke, P. B. Hitchcock, J. Leonard, A. K. de K. Lewis, D. McKerrecher, L. R. Titcomb, *Organometallics* **2002**, *21*, 4318–4319; b) A. K. de K. Lewis, S. Caddick, F. G. N. Cloke, N. C. Billingham, P. B. Hitchcock, J. Leonard, *J. Am. Chem. Soc.* **2003**, *125*, 10066–10073; c) A. K. de K. Lewis, S. Caddick, O. Esposito, F. G. N. Cloke, P. B. Hitchcock, *Dalton Trans.* **2009**, 7094–7098.
[13] a) T. Schaub, M. Backes, O. Plietzsch, U. Radius, *Dalton Trans.* **2009**, 7071–7079; b) T. Schaub, M. Backes, U. Radius, *Eur. J. Inorg. Chem.* **2008**, 2680–2690; c) T. Schaub, M. Backes, U. Radius, *Chem. Commun.* **2007**, 2037–2039; d) T. Schaub, U. Radius, *Chem. Eur. J.* **2005**, *11*, 5024–5030.
[14] a) J. C. Green, B. J. Herbert, R. Lonsdale, *J. Organomet. Chem.* **2005**, *690*, 6054–6067; b) J. C. Green, B. J. Herbert, *Dalton Trans.* **2005**, 1214–1220.
[15] R. B. Jordan, *Organometallics* **2007**, *26*, 4763–4770.
[16] a) F. Ozawa, T. Ito, Y. Nakamura, A. Yamamoto, *J. Organomet. Chem.* **1979**, *168*, 375–391; b) Y.-J. Kim, K. Osakada, A. Takenaka, A. Yamamoto, *J. Am. Chem. Soc.* **1990**, *112*, 1096–1104.
[17] Y.-J. Kim, S.-W. Song, S.-C. Lee, S. W. Lee, K. Osakada, T. Yamamoto, *J. Chem. Soc., Dalton Trans.* **1998**, 1775–1779.
[18] a) L. R. Titcomb, S. Caddick, F. G. N. Cloke, D. J. Wilson, D. McKerrecher, *Chem. Commun.* **2001**, 1388–1389; b) K. Arentsen, S. Caddick, F. G. N. Cloke, A. P. Herring, P. B. Hitchcock, *Tetrahedron* **2004**, *45*, 3511–3515.
[19] a) V. P. W. Böhm, C. W. K. Gstöttmayr, T. Weskamp, W. A. Herrmann, *J. Organomet. Chem.* **2000**, *595*, 186–190; b) C. W. K. Gstöttmayr, V. P. W. Böhm, E. Herdtweck, M. Grosche, W. A. Herrmann, *Angew. Chem. Int. Ed.* **2002**, *41*, 1363–1365.
[20] S. Fantasia, S. P. Nolan, *Chem. Eur. J.* **2008**, *14*, 6987–6993.
[21] a) T. Ito, H. Tsuchiya, A. Yamamoto, *Bull. Chem. Soc. Jpn.* **1977**, *50*, 1319–1327; b) F. Ozawa, A. Yamamoto, *J. Am. Chem. Soc.* **1980**, *102*, 6457–6463; c) A. Yamamoto, *J. Organomet. Chem.* **1986**, *300*, 347–367.
[22] J. M. Wisner, T. J. Bartczak, J. A. Ibers, *Organometallics* **1986**, *5*, 2044–2050.
[23] W. de Graaf, J. Boersma, W. J. J. Smeets, A. L. Spek, G. van Koten, *Organometallics* **1989**, *8*, 2907–2917.
[24] P. Leoni, *Organometallics* **1993**, *12*, 2432–2434.
[25] a) R. McCrindle, G. Ferguson, A. J. McAlees, G. J. Arsenault, A. Gupta, M. C. Jennings, *Organometallics* **1995**, *14*, 2741–2748; b) R. McCrindle, G. J. Arsenault, R. Farwaha, A. J. McAlees, D. W. Sneddon, *J. Chem. Soc., Dalton Trans.* **1989**, 761–766.
[26] H. Günther, *NMR Spectroscopy: An Introduction*, Wiley, New York, **1980**.
[27] J. Kermode, M. F. Lappert, *J. Chem. Soc., Chem. Commun.* **1981**, 698–699.
[28] C. A. Ghilardi, S. Midollini, A. Oriandini, J. A. Ramirez, *J. Chem. Soc., Chem. Commun.* **1989**, 304–306.
[29] O. J. Scherer, H. Jungmann, *J. Organomet. Chem.* **1981**, *208*, 153–159.
[30] P. K. Monaghan, R. J. Puddephatt, *Organometallics* **1985**, *4*, 1406–1412.
[31] M. Huser, M.-T. Youinou, J. A. Osborn, *Angew. Chem. Int. Ed. Engl.* **1989**, *28*, 1386–1388.
[32] A. L. Balch, C. T. Hunt, C.-L. Lee, M. M. Olmstead, J. P. Farr, *J. Am. Chem. Soc.* **1981**, *103*, 3764–3772.
[33] J. V. Caspar, *J. Am. Chem. Soc.* **1985**, *107*, 6718–6719.
[34] H. Werner, W. Paul, *J. Organomet. Chem.* **1982**, *236*, C71–C74.
[35] E. G. Burns, S. S. C. Chu, P. de Meester, M. Lattman, *Organometallics* **1986**, *5*, 2383–2384.
[36] T. B. Marder, W. C. Fultz, J. C. Calabrese, R. L. Harlow, D. Milstein, *J. Chem. Soc., Chem. Commun.* **1987**, 1543–1545.
[37] P. J. Fennis, P. H. M. Budzelaar, J. H. G. Frijns, A. G. Orpen, *J. Organomet. Chem.* **1990**, *393*, 287–298.
[38] M. A. Ciriano, M. A. Tena, L. A. Oro, *J. Chem. Soc., Dalton Trans.* **1992**, 2123–2124.
[39] K. Kashiwabara, A. Morikawa, T. Suzuki, K. Isobe, K. Tatsumi, *J. Chem. Soc., Dalton Trans.* **1997**, 1075–1081.
[40] J. Y. Zeng, M.-H. Hsieh, H. M. Lee, *J. Organomet. Chem.* **2005**, *690*, 5662–5671.
[41] a) J. Ito, T. Miyakwa, H. Nishiyama, *Organometallics* **2006**, *25*, 5216–5218; b) H. Nishiyama, M. Horihata, T. Hirai, S. Wakamatsu, K. Itoh, *Organometallics* **1991**, *10*, 2706–2708; c) J. Ito, T. Miyakawa, H. Nishiyama, *Organometallics* **2008**, *27*, 3312–3315.
[42] C. Tejel, M. A. Ciriano, L. A. Oro, A. Tiripicchio, F. Ugozzoli, *Organometallics* **2001**, *20*, 1676–1682.
[43] G. E. Ball, W. R. Cullen, M. D. Fryzuk, B. R. James, S. J. Rettig, *Organometallics* **1991**, *10*, 3767–3769.
[44] J. Chang, R. G. Berman, *J. Am. Chem. Soc.* **1987**, *109*, 4298–4304.
[45] D. A. Freeman, K. R. Mann, *Inorg. Chem.* **1991**, *30*, 836–840.
[46] C. Tejel, M. A. Ciriano, S. Jimenz, L. A. Oro, C. Graiff, A. Tiripicchio, *Organometallics* **2005**, *24*, 1105–1111.

[47] J. A. Labinger, J. A. Osborn, N. Coville, *Inorg. Chem.* **1980**, *19*, 3236–3243.
[48] W. L. Olson, D. A. Nagaki, L. F. Dahl, *Organometallics* **1986**, *5*, 630–634.
[49] H. H. Murray, J. P. Fackier Jr., A. M. Mazany, *Organometallics* **1984**, *3*, 1310–1311.
[50] W. J. Marshall, V. V. Grushin, *Organometallics* **2003**, *22*, 1591–1593.
[51] L. Jafarpour, E. D. Stevens, S. P. Nolan, *J. Organomet. Chem.* **2000**, *606*, 49–54.
[52] G. T. L. Broadwood-Strong, P. A. Chaloner, P. B. Hitchcock, *Polyhedron* **1993**, *12*, 721–729.
[53] G. M. Sheldrick, *SADABS*, Program for Absorption Correction, University of Göttingen, **1996**.
[54] Bruker, *SHELXTL*, Structure Determination Software Programs, Bruker Analytical X-ray Instruments Inc., Madison, Wisconsin, USA, **1997**.

Received: December 2, 2010
Published Online: March 4, 2011

